Tailings Improvement by Stress-Densification from Waste Rock Capping

Thomas E. Sully, M.S.E., P.Eng.
Knight Piésold Ltd., Vancouver, British Columbia, Canada

Ken Brouwer, P.Eng., P.E.
Knight Piésold Ltd., Vancouver, British Columbia, Canada

Peter K. Robertson, Ph.D., P.E.
PK Robertson Inc., Newport Beach, California, USA

Graham Greenaway, P.Eng.
Knight Piésold Ltd., Vancouver, British Columbia, Canada

ABSTRACT: Long-term risks associated with slurry tailings facilities are often related to the requirement for long-term containment of loose, saturated, and potentially fluid tailings. Saturated loose tailings have been known to liquefy with highly fluid mudflow events occurring after a tailings storage facility (TSF) breach, despite the absence of surface water ponding.

Risks associated with long-term tailings storage can be mitigated through the appropriate application of in-situ tailings improvement techniques, such as stress-densification, which can be a relatively economic ground improvement technology for low-density saturated tailings deposits. Stress-densification results when increased effective stresses cause consolidation of the tailings mass with an associated reduction in the moisture content, brittleness and potential mobility of liquefiable tailings.

Two 30 m high test pads were constructed by selectively placing waste rock on the surface of the decommissioned Candelaria TSF. The test pads were sized to replicate the loading that would be caused by construction of a thick, gently sloping waste rock closure cap, and evaluate tailings improvements relating to stress densification.

Site investigations were carried out before and after test pad construction to assess changes to the in-situ state and strength characteristics of the tailings. The field investigations were supplemented with specialized laboratory testing which quantified the effect of increasing confining pressure on the shape of the critical state line and demonstrated improvement in the undrained shear strength of the tailings.

The trial program demonstrates the efficacy of surcharge loading to stabilize and improve the residual shear strength characteristics of in-situ tailings. Improving the tailings shear strength properties can mitigate risks related to long-term tailings containment.

1 INTRODUCTION

The Candelaria Mine is an active open pit copper mine operated by Compañía Contractual Minera Candelaria located in the Atacama region of Chile, 20 km south of Copiapó. The Candelaria Tailings Storage Facility (TSF) was deactivated in 2018 and a surface cap is planned for closure of the impoundment. Continued mining will generate approximately 800 Mt of waste rock during ongoing open pit mining operations, and the decommissioned TSF provides an opportunity for closure capping activities to be integrated with long term waste rock disposal during ongoing mine operations. The closure cap will be constructed on the surface of the TSF by progressive placement of waste rock in layers to develop a 20m to 60m thick waste rock cap with flat (20H:1V) overall slopes, as shown schematically on Figure 1. Capping the Candelaria TSF will provide significant storage capacity for waste rock within a reasonable haulage distance from the open pit and will reduce additional site disturbances for ongoing mine operations.

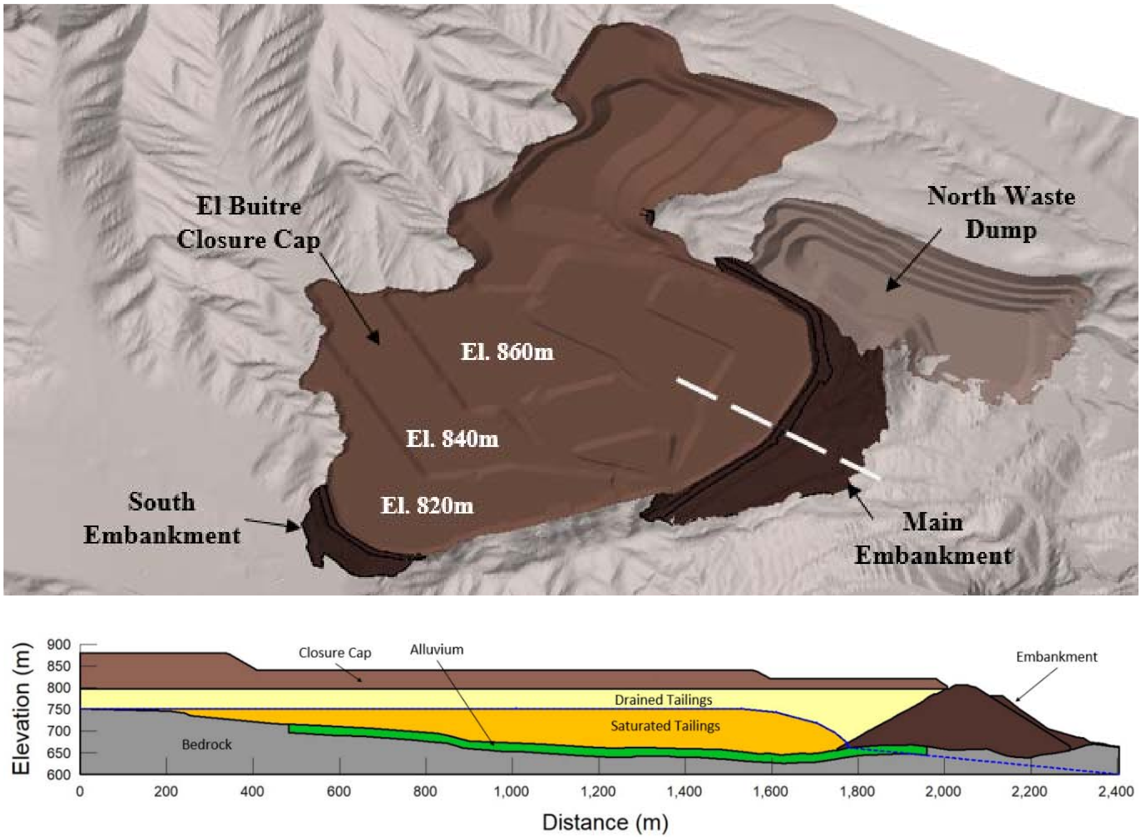

Figure 1. Plan and section of the proposed closure cap on the Candelaria TSF.

From a technical design perspective, the large quantities of future waste rock will allow the mine to construct a thick, gently sloping closure cap on the tailings which has been designed to improve the characteristics of the loose, contractive near-surface tailings; and to facilitate post-closure surface water management by providing a naturally appearing convex, free-draining, stable post-closure landform. The design team indicated that the waste rock cap should be constructed as thick as practical to sufficiently increase the stress state of the tailings and reduce strength loss potential of the tailings during undrained shear – which ultimately increases the overall stability of the impoundment and reduces the risk associated with a hypothetical dam breach of the facility. The design philosophy was largely rooted on the concepts presented by Robertson (2017).

Proof-of-concept field and laboratory testing programs were developed to verify the ability to construct the waste rock cap and demonstrate the long-term benefits of surcharge loading on the impounded tailings (Sotil et al., 2020). The field component comprised of evaluating the in-situ state and strength characteristics of the tailings at closure and after construction of two 30 m high waste rock test pads, which were sized to replicate the loading imposed by construction of the proposed waste rock closure cap. In-situ characterization of the tailings was primarily carried out by advancing a series of seismic cone penetration tests (SCPT) to depths of approximately 80 m below the tailings surface. The SCPT data collected before pad construction provided baseline conditions and properties for "unimproved tailings" and were also used to specify the geometry and construction sequence of the test pads. The pre-construction site investigation (SI) also provided the opportunity to install instrumentation to measure the performance of the tailings during construction. Post construction test pad SCPTs were then advanced through the test pad fill to evaluate the change in tailings properties after construction-induced excess pore water pressures were fully dissipated.

The field data were supplemented with specialized laboratory testing which quantified the effect of increased confining pressure. The laboratory testing program was developed using a critical state soil mechanics approach to determine how stress densification could reduce the strength loss potential and ultimately reduce the risks associated with long-term storage of the tailings (Adams et al., 2022; Castellanos et al., 2022).

This paper summarizes the main results from the field and laboratory testing that show improvements in tailings behavior due to an increase in in-situ stress state. The results of this proof-of-concept test program support the use of stress densification as at an effective tailings improvement method at this site.

2 STRESS DENSIFICATION CONCEPT

Recent failures of mine tailings structures have highlighted the importance of the undrained strength and behavior of loose tailings. Loose, saturated tailings can experience significant and rapid strength loss if triggered to behave undrained under shear and this process has been described as either flow or static liquefaction. A flow (static) liquefaction failure is due to a significant and rapid strength loss in undrained shear that can occur in any saturated or near saturated loose soil, such as very loose sands and silts, and is a major design consideration for large soil structures such as mine tailings impoundments.

Several recent failures of tailings impoundments have shown that when significant and rapid strength loss occurs in critical sections of a soil structure, the resulting failure is often rapid, and occurs with little warning; and the resulting deformations are often very large (e.g., Morgenstern et al., 2016, Robertson et al., 2019). Case histories involving flow liquefaction failures also show that the initial effective confining stress prior to strength reduction was less than 300kPa and mostly less than 200kPa.

Robertson (2017) laid out a framework to show that increasing effective confining stress can decrease the potential for strength loss in loose, saturated tailings when subjected to undrained shear. The key element in this framework is the observation that the critical state line (CSL) is curved at high effective confining stresses and that the curvature is a function of grain characteristics, such as fines content and mineralogy. This is consistent with the observations made by others (e.g., Jefferies and Been, 2016) that show that the slope of the CSL has an important role in the behavior of contractive soils. At higher effective confining stresses, the curvature of the CSL results in a steeper slope to the CSL with a resulting reduction in potential strength loss. Hence, increasing the effective confining stress can produce denser tailings with less strength loss potential.

This concept is illustrated in Figure 2 using data for Erksak sand (Jefferies and Been, 2016). Erksak sand is a uniform clean silica sand, where the CSL becomes highly non-linear at high stresses and the slope of the CSL approaches values like either compressible sand-like soils (e.g., carbonate sands) or clay-like soils. Jefferies and Been (2016) did sufficient testing on Erksak sand to also define the Limiting Compression Curve (LCC) that is also shown in Figure 2. Figure 2 shows the start and end points for three example isotropically consolidated undrained triaxial compression tests performed on reconstituted samples from very loose states. Full details and associated test results are contained in Jefferies and Been (2016). The slope of the CSL (denoted as M) at the critical state (CS) for Erksak sand (in triaxial compression) is $M_{tc} = 1.2$ (i.e., $\phi'_{cs} = 30^0$).

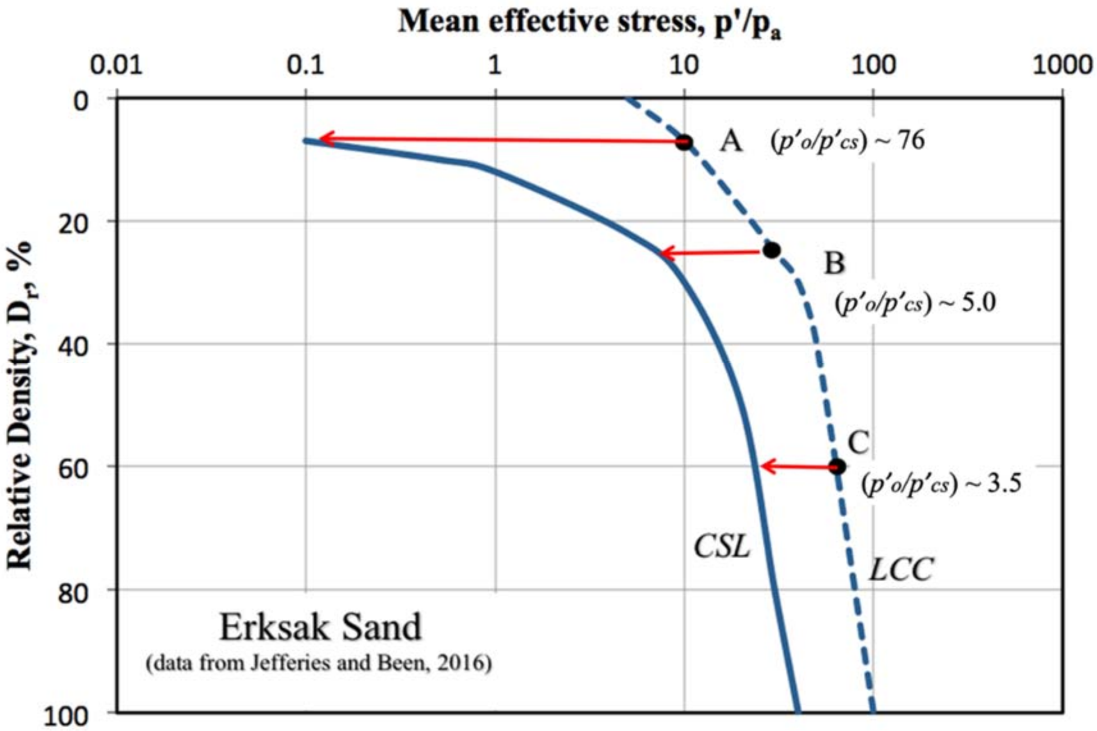

Figure 2. Critical State Line (CSL) and approximate Limiting Compression Curve (LCC) for Erksak sand (data from Jefferies and Been, 2016).

A summary of the results from the three isotropically consolidated undrained triaxial compression tests are shown in Table 1.

Table 1. Summary of isotropically consolidated undrained triaxial compression tests results on Erksak sand (Jefferies and Been, 2016).

Test	ψ	p'_o/p_a	p'_o/p'_{cs}	$Su_{(cs)}/\sigma'_{vo}$	I_{SL}
A	0.07	10	76	0.008	0.96
B	0.20	30	5.0	0.12	0.45
C	0.25	60	3.5	0.17	0.23

Where:

ψ	State parameter
p'_o	Current in-situ mean effective stress;
p'_{cs}	Mean effective stress at CS for the same void ratio
$Su_{(cs)}$	Residual undrained shear strength at Critical State (i.e. large strains)
σ'_{vo}	In-situ vertical effective stress
I_{SL}	Strength Loss Index (same as Brittleness Index by Bishop, 1967)

The data in Table 1 show that the initial state parameter is not a good index of undrained behavior, unless the slope of the CSL is included. The results also show that with increasing effective confining stress, Erksak sand experiences less stress loss (i.e., decreasing ISL) in undrained loading. Data from tailings and other soils, show that more compressible soils (e.g., silty sand tailings) develop increased curvature of the CSL at lower stresses than the less compressible Erksak sand.

Increasing the effective confining stress (stress densification) can be achieved in various ways, the most common being the application of a surcharge load using fill material.

3 TEST PAD CONSTRUCTION

An overview of the Candelaria TSF and Test Pad locations is shown on Figure 3.

Figure 3. Overview of Candelaria TSF showing Test Pad locations.

The Test Pads had a central diameter at the crest of about 70m with average side slopes of 2H:1V, over a 6m thick base of about 280m in diameter, as shown by the aerial photo in Figure 4. Test Pad 1 was constructed on a relatively competent area of the coarser tailings beach, and Test Pad 2 was constructed on finer grained saturated tailings adjacent to the historical reclaim water pond. The Test Pads experienced total settlement of about four meters at Test Pad 1 and six meters at Test Pad 2. Settlements and excess pore pressure dissipation from pad loading were complete within four months after pad construction.

Figure 4. Aerial view of the Candelaria Test Pads.

4 TAILINGS CHARACTERIZATION

The Candelaria tailings were hydraulically deposited from the perimeter of the impoundment and are generally layered and segregated, with coarser (sandier) materials more prominent near the discharge points and the tailings becoming finer (siltier) farther from the perimeter, towards the historical reclaim water pond. Site investigations were scoped to evaluate the in-situ condition and material properties of both the sandier perimeter tailings and the finer-grained tailings near the reclaim pond.

Site investigations were completed on the surface of the deactivated tailings impoundment before and after construction of the Test Pads, with the investigations focused on evaluating tailings improvements due to loading, including changes in the undrained shear strength properties of the tailings. The site investigations at the Test Pads incorporated sonic drilling, sample collection, installation of vibrating wire piezometers and SCPT investigations. The post-loading SCPTs and drillholes were carried out after construction-induced excess pore pressures were fully dissipated.

The equilibrium pore pressure conditions in the tailings were determined from vibrating wire piezometer (VWP) measurements and SCPT pore pressure dissipation (PPD) tests. The equilibrium pore pressure profiles were determined during Phase 1 (before pad construction) and Phase 2 (after pad construction) site investigation programs. In general, the tailings were found to be draining downwards towards the pervious basal alluvium deposit, with pore pressure conditions found to be significantly less than hydrostatic. Active drain-down was also measured by the VWP instrumentation during the 2-year construction and monitoring period, with a drop in the phreatic surface measured at approximately 0.5 meters/month at both Test Pad locations. The drain-down is also evident in the piezometric profiles that were developed before and after construction of the Test Pads. The equilibrium pore pressure profiles were used to determine effective stresses within the tailings at the time of each investigation.

SCPT profiles were obtained in the tailings at both Test Pad locations before and after pad construction. Example SCPT profiles (Before and After) are shown on Figures 5 (Test Pad 1) and Figure 6 (Test Pad 2) and illustrate profiles of the tip resistance (q_t), normalized cone resistance (Q_{tn}), shear wave velocity (V_s), and normalized shear wave velocity (V_{s1}) by elevation, to examine the improved tailings response after pad construction. The normalized cone-resistance values were filtered as mean values over one-meter intervals to reduce the scatter in the data.

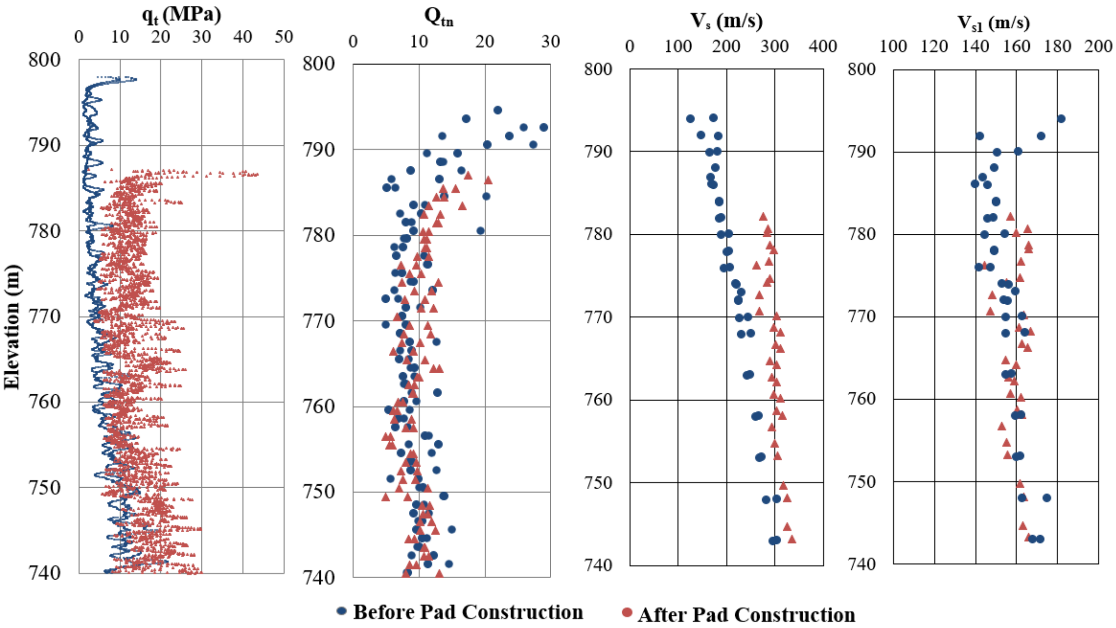

Figure 5. SCPT data before and after construction of Test Pad 1.

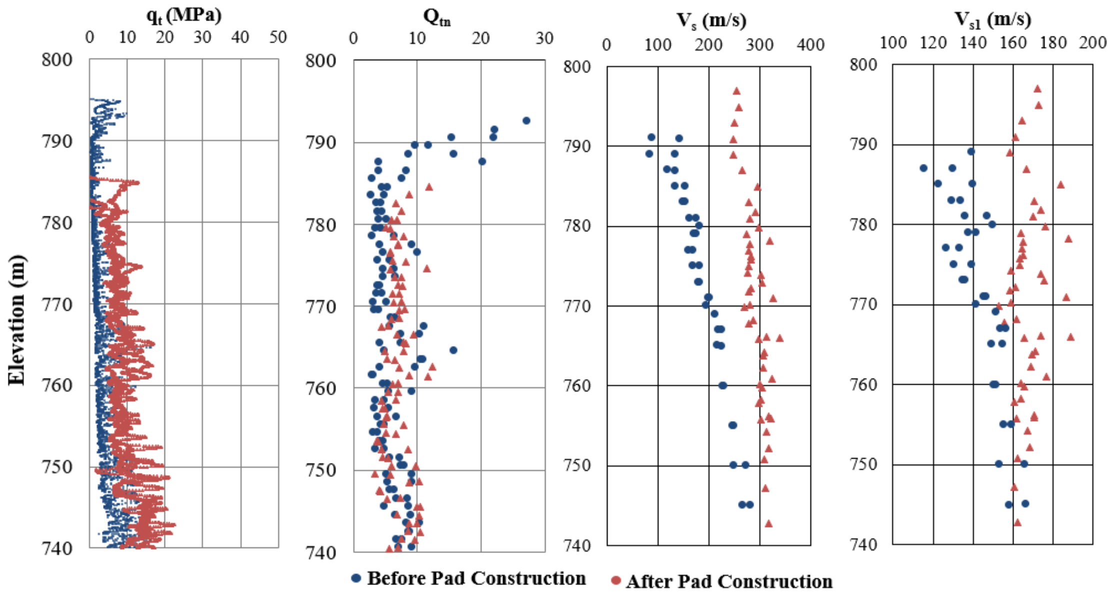

Figure 6. SCPT data before and after construction of Test Pad 2.

The SCPT data recorded at both Test Pad locations show significant increases in the tailings resistance and stiffness after Test Pad construction. Increases in confining stress would be expected to result in an increase in the material stiffness, as reflected in the raw tip and shear wave veolocity measurements. However, the SCPT data also show an increase in the stress-nomalized tip resistance and shear wave velocity measurements above elevation (EL.) 760 m, which indicates an improvement in the in-situ density and state of the shallower tailings. Q_{tn} values in the upper 30m of saturated tailings generally increased after Test Pad construction from 7 to 12 and from 4 to 7 at Test Pad 1 and 2, respectively. Robertson (2022) presented a revised methodology for estimating the residual undrained shear strength ratio for contractive materials using the SCPT measured Q_{tn} parameter corrected for soil compressibility. Therefore, the increase in Q_{tn} values indicates that surcharge loading resulted in an increase in the residual undrained shear strength ratio for the tailings materials. The relative changes in Q_{tn} were greater for the finer tailings encountered at Test Pad 2 suggesting a larger improvement in the tailings residual strength ratio relative to the coarser tailings at Test Pad 1.

The combined shear wave velocity (Vs) and CPT data indicate that the tailings have no micro-structure based on the methodology suggested by Robertson (2016) where the average K^*_G (normalized rigidity index) values are around 200. Given the lack of any microstructure in the tailings, the updated method suggested by Robertson (2022) was considered appropriate for estimating the large strain residual undrained strength ratio of the contractive tailings.

Interpretation of the tailings state parameter was carried out using the approach proposed by Robertson (2022) and indicated that the tailings at both test pad sites were loose, as expected, with slightly higher (looser) state parameter values observed at the Test Pad 2 location. State parameter values generally varied between -0.05 and 0.01 at Test Pad 1 and -0.05 to 0.06 at Test Pad 2.

Robertson (2022) presented contour lines of the residual undrained strength ratio on the normalized Soil Behavior Type (SBT_n) as illustrated on Figures 7 and 8. The SBT_n chart includes the CD = 70 line which provides an approximate boundary between contractive (below the CD = 70 line) and dilative materials (above the CD = 70 line). In general, materials plotting below but near the CD = 70 line have higher residual undrained shear strengths than materials that plot further below the boundary. The SCPT data collected at Test Pad 1 and Test Pad 2 are plotted as point density contours on the SBT_n charts on Figures 7 and 8. The SCPT data were filtered to only include approximately the upper 30m of the saturated tailings at each Test Pad, as these are the loosest materials that experience the largest incremental change after Test Pad construction. As expected, the tailings at both test pad locations plot below the CD=70 further confirming that they are contractive, with the Test Pad 1 tailings typically plotting nearer to the contractive-dilative boundary. The Test Pad 2 data plots further down and right of the Test Pad 1 data indicating that the tailngs at the Test Pad 2 location are finer and more compressible.

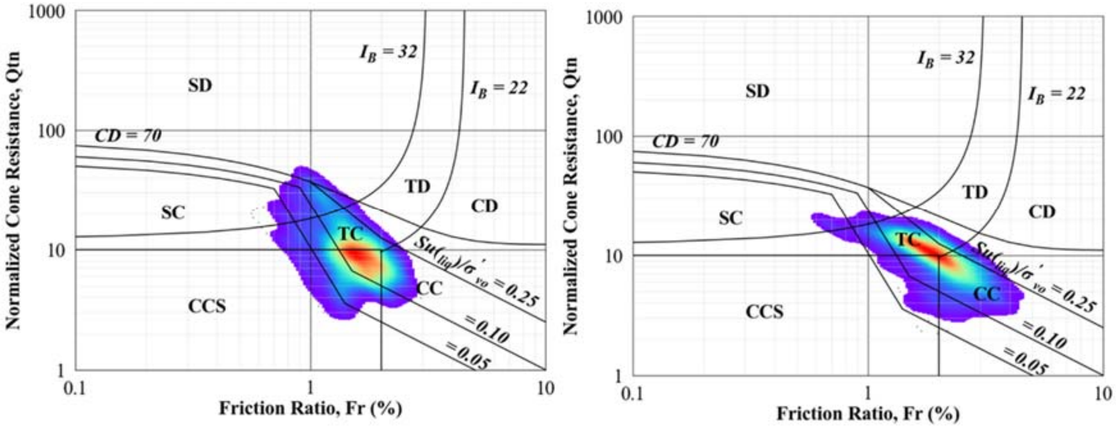

Figure 7. SBTn plots for Test Pad 1 with contours of $Su_{(liq)}/\sigma'_{vo}$ before (left) and after (right) Test Pad loading (for saturated tailings above EL. 763m).

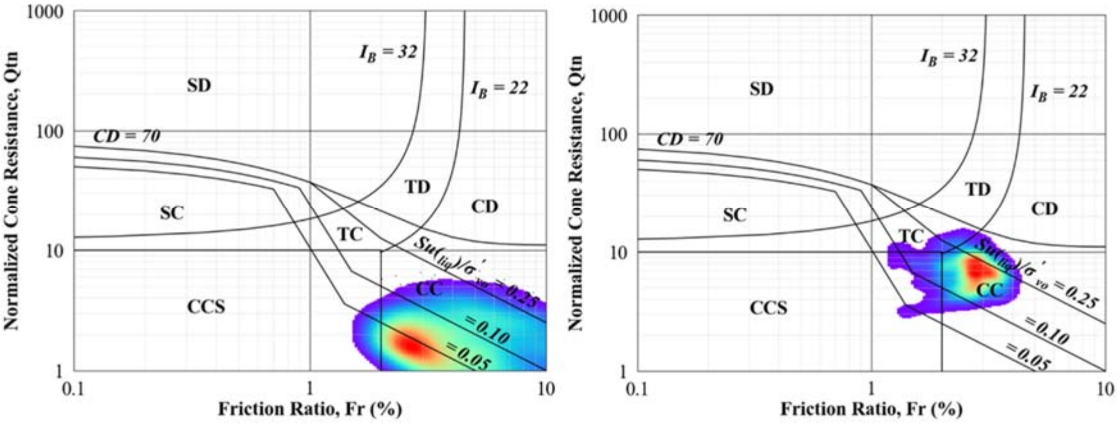

Figure 8. SBTn plots for Test Pad 2 with contours of $Su_{(liq)}/\sigma'_{vo}$ before (left) and after (right) Test Pad loading (for saturated tailings above EL 763m).

The SBT_n point density contours show the improvement in the residual undrained shear strength ratio of the tailings after loading, further supporting the observations made from the SCPT profiles presented on Figures 5 and 6. Figure 7 shows the loosest SCPT data points at Test Pad 1 shifting upwards towards the CD=70 contractive-dilative boundary after surcharge loading. The upwards shift indicates that the loose tailings layers below Test Pad 1 were improved and densified by the surcharge load. Figure 8 shows a more pronounced change in the SBT_n isopach at Test Pad 2, which is reasonable given the initial looser state of the finer tailings located closer to the historical reclaim pond area. The mean residual undrained shear strength ratio estimated from these SBT_n plots is shown to have increased from approximately 0.13 to 0.2 at Test Pad 1 and from 0.04 to 0.2 at Test Pad 2.

5 LABORATORY VERIFICATION

The sampling program included grab and tube sampling to enable index testing on the tailings prior to defining specialized laboratory testing to evaluate the CSL and undrained strength characteristics of the tailings.

Particle size distribution, Atterberg Limits, and X-ray diffraction testing indicated that the Candelaria tailings are essentially non-plastic silty sand to sandy silt with a mineralogy composed of about 15 to 20% quartz, 35% feldspar minerals, 30 to 40% mica/chlorite, with 5 to 8 % clay (smectite). Samples retrieved from the Test Pad 1 and Test Pad 2 locations were blended to evaluate the undrained strength properties of the coarse-grained and fine-grained portion of the tailings.

The particle size distributions for multiple tailings samples collected from various depths at Test Pads 1 and 2 are illustrated on Figure 9. Laboratory tailings samples were prepared by selectively separating and blending tailings to generate Coarse sandy tailings and Fine silty tailings samples, as highlighted on Figure 9. The individual reconstituted samples are not strictly representative of the in-situ layered tailings materials below the two test pads but provide general bounding conditions for the CSL laboratory testing. In general, the Coarse sandy tailings were intended to be more representative of the predominant materials under Test Pad 1 and the Fine silty tailings more representative of the predominant materials under Test Pad 2. The individual particle size distribution curves show that the Candelaria tailings are relatively well graded. Laboratory strength testing was completed on each of the two sample blends to define the CSL and evaluate the impact of confining stress on the minimum undrained shear strength of the tailings.

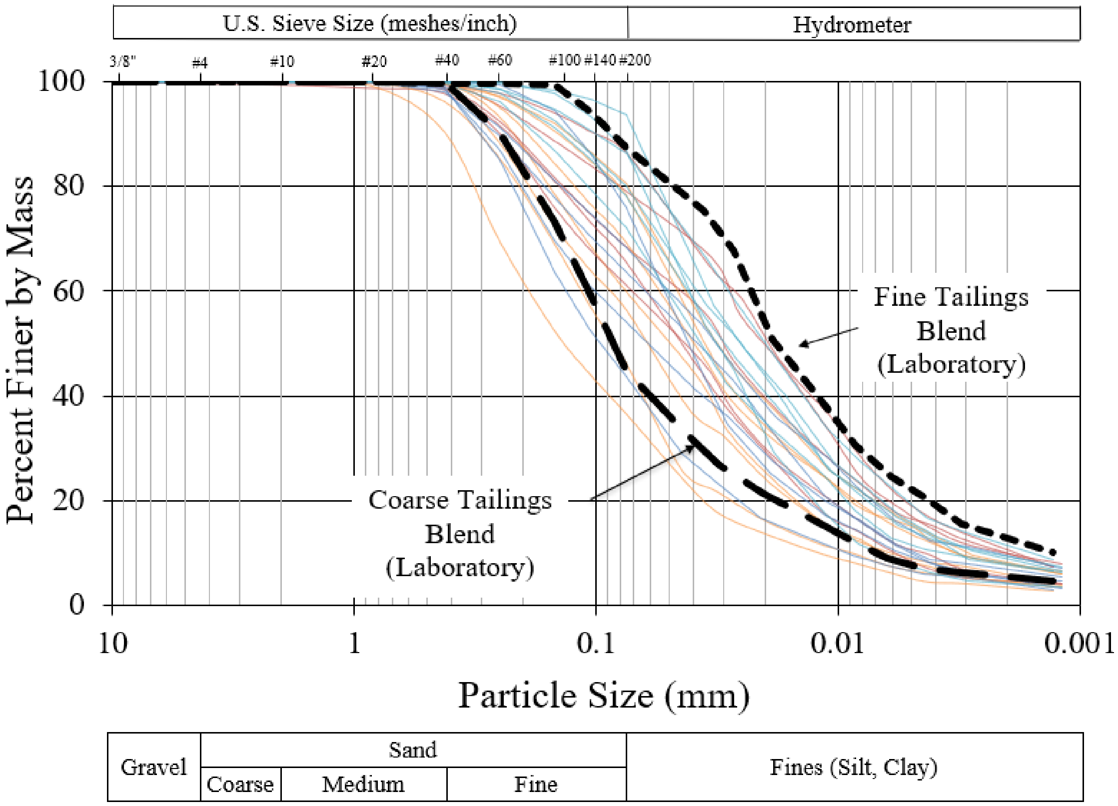

Figure 9. Candelaria tailings gradation envelope with representative reconstituted laboratory samples.

The Coarse and Fine tailings samples were prepared to the loosest possible state (using moist tamping) and subjected to isotropically consolidated undrained triaxial compression testing to define the CSL at low and high stresses, as illustrated on Figure 10. Included on Figure 10 are the estimated Limiting Compression Curves (LCC) that represent the loosest state obtained in the laboratory for the reconstituted samples. Bender element tests were carried out during isotropic consolidation on two of the triaxial test samples to assist with developing the LCC. When possible, the triaxial samples were frozen after shearing to accurately measure the void ratio of the sample.

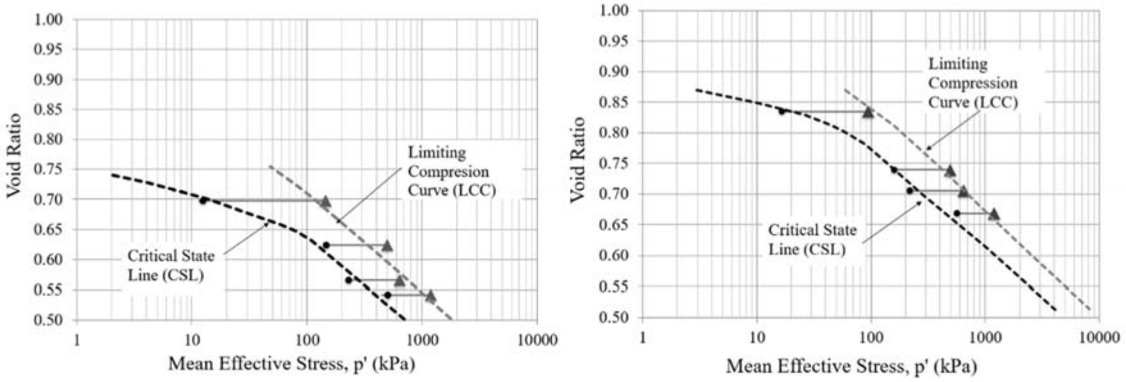

Figure 10. Curved CSLs for Coarse (left) and Fine (right) laboratory tailings samples.

Triaxial compression test results were used to develop curved CSLs, LCCs, and the slope of the CSL (M_{tc}) for both the Coarse and Fine tailings by measuring the stress path during shearing. The offset between the LCC and the CSL were used to calculate the minimum undrained shear strength ratio at CS ($Su_{(min)}/\sigma'_{vo}$) over a wide stress range for the Candelaria tailings and are compared to the lines for Erksak sand and a silty gold tailings (Schnaid et al., 2013), as shown on Figure 11. The curves developed for the Candelaria tailings are very similar to the silty gold tailings, with the Fine tailings (80% fines content) plotting slightly to the left and the Coarse tailings (40% fines content) plotting slightly to the right of the reference silty gold tailings (40% fines content). Based on the similar mineralogy and fines content between the Candelaria tailings and the Schnaid silty gold tailings (see Table 2), it is reasonable to expect good agreement between these curves.

Table 2. Summary of the main characteristics of the materials shown on Figure 11.

Sand	D_{50} (mm)	Fines content (%)	Main minerals	Specific gravity (G_s)	References
Erksak sand	0.33	< 1	Quartz	2.7	Jefferies and Been (2016)
Silty (gold) tailings	0.10	~40%	Quartz (32%) Albite (24%) Chlorite (23%)	3.0	Schnaid et al. (2013)
Coarse tailings (Candelaria)	0.10	40% (includes 5% clay size)	Quartz (17%) Feldspars (35%) Mica/Chlorite (35%)	3.0	Sotil et al. (2020)
Fine tailings (Candelaria)	0.03	82% (includes 12% clay size)	Quartz (19%) Feldspars (36%) Mica/Chlorite (30%)	3.0	Sotil et al. (2020)

A small number of constant volume direct simple shear (DSS) tests were also carried out on the Candelaria tailings at two effective vertical consolidation stresses (500 kPa and 1,000 kPa). The values of the minimum undrained shear strength ratio from the DSS tests were about 20% lower than those from the triaxial compression tests which is consistent with other published data for non-plastic sands and silts at the differing modes of shear. The DSS test results are also plotted on Figure 11. The SCPT interpreted mean residual undrained strength relationships from Test Pad 1 and Test Pad 2 are also included on Figure 11 to compare the field and laboratory derived data.

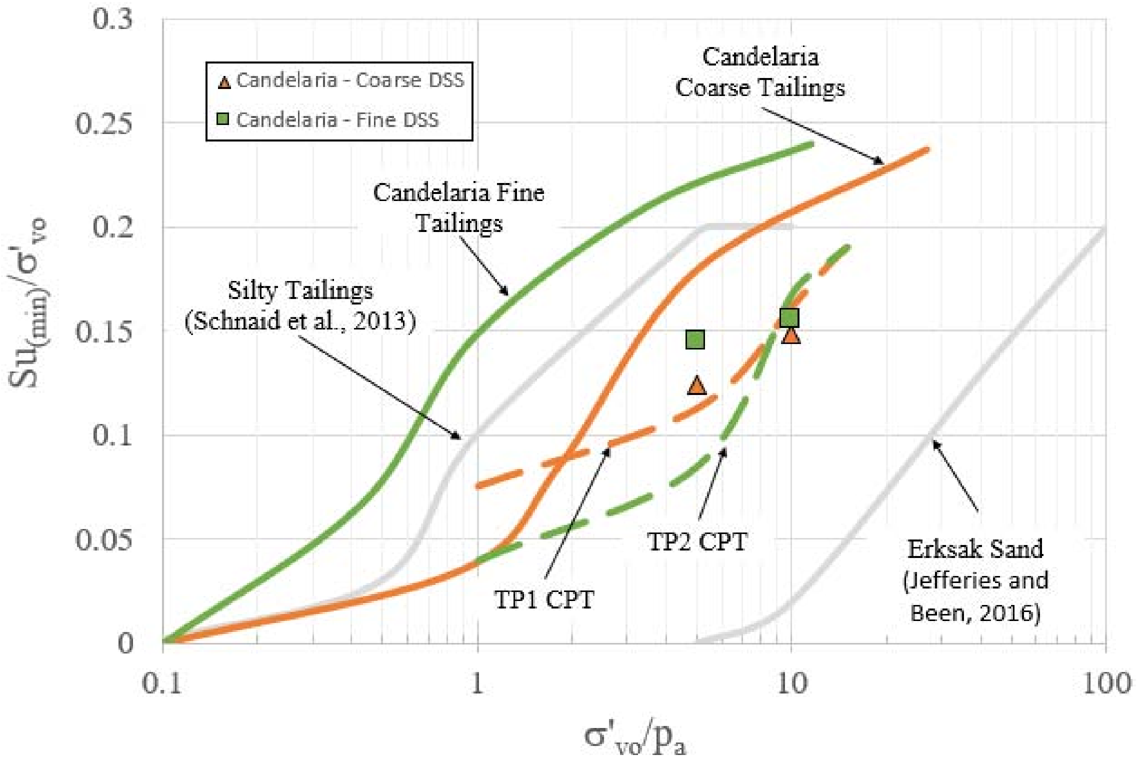

Figure 11. Variation of $Su_{(min)}/\sigma'_{vo}$ for Candelaria tailings as a function of normalized effective confining stress (σ'_{vo}/p_a), (with reference to Erksak sand and Schnaid silty tailings).

Figure 11 compares the laboratory and SCPT results from the Candelaria Test Pads relative to previously published trends. The SCPT interpreted values agree very well with the limited DSS test results. The SCPT residual undrained shear strength equations (Robertson, 2022) were developed mainly from back-analyses of past case histories where failure modes tend to be dominated by the DSS direction of loading which may explain the generally good agreement observed. It is encouraging that the SCPT-based correlations worked well over the wide stress range at this site. The Candelaria tailings have similar grain characteristics to the silty gold tailings tested by Schnaid et al. (2013) and the results show a very similar trend.

6 CONCLUSIONS

Two large rockfill Test Pads were constructed over the Candelaria tailings to evaluate the benefits from stress densification. SCPT and laboratory testing provided data to evaluate the influence of stress densification on the large strain undrained shear strength of loose tailings. Results were analyzed using the framework suggested by Robertson (2017) using a Critical State approach. The laboratory data on the Candelaria tailings show that the CSL is non-linear over a wide stress range and that the non-linearity plays an important role in characterizing the undrained strength behavior. Laboratory testing on the Candelaria tailings also showed that the undrained strength ratio in DSS loading is lower than that observed in triaxial compression loading, which is consistent with past research.

The Candelaria case history provides valuable SCPT data from the underlying tailings materials, both before and after loading from the test pads. The SCPT data were interpreted using the updated approach by Robertson (2022) and showed trends consistent with the laboratory data, especially with respect to the DSS results. Good agreement between the SCPT and DSS data is encouraging, as the Robertson (2022) interpretation method is based primarily on past case history failures where DSS is likely the dominant loading condition. Field and laboratory data collected at the Candelaria TSF demonstrate that stress densification using surcharge loading can be an effective means to enhance the residual undrained shear strength of the tailings.

7 REFERENCES

Adams, A.L., Brouwer, K., Robertson, P.K., and Martin, V., 2022. Evaluation of Tailings Behviour for Dam Breach Analysis. Tailings and Mine Waste Conference, Denver, Colorado. November. (Citation Adams et al., 2022)

Castellanos, J., Yong, S., and Martin, V., 2022. Application of 3D Limit Equilibrium Method in Tailings Dam Breach Analysis. Tailings and Mine Waste Conference, Denver, Colorado. November. (Citation Castellanos et al., 2022)

Jefferies, M.G., and Been, K. 2016. Soil liquefaction – a critical state approach. *Taylor & Francis*, London, ISBN 0-419-16170-8 478 pages.

Morgenstern, N.R., Vick, S., Viotti, C.B., and Watts, B.D. (2016). "Report on the immediate causes of the failure of the Fundao Dam." Fundao Tailings Dam Review Panel http://fundaoinvestigation.com.

Robertson, P.K. 2010. Evaluation of flow liquefaction and liquefied strength using the cone penetration test. *Journal of Geotechnical and Geoenvironmental Engineering*, ASCE, 136(6): 842–853.

Robertson, P.K. 2016. Cone Penetration Test (CPT)-based soil behavior type (SBT) classification system – an update. *Canadian Geotechnical Journal*, 53(12).

Robertson, P.K. 2017. Evaluation of flow liquefaction: influence of high stresses. Keynote presentation PDB-III Earthquake Geotechnical Engineering, Vancouver, BC.

Robertson, P.K. 2021. Evaluation of flow liquefaction and liquefied strength using the cone penetration test: an update. *Canadian Geotechnical Journal*. https://doi.org/10.1139/cgj-2020-0657.

Robertson, P.K., de Melo, L., Williams, D.J., and Wilson, G.W. (2019). "Report of the expert panel on the technical causes of the failure of Feijao Dam 1." http://www.b1technicalinvestigation.com.

Schnaid, F., Bedin, J., Viana da Fonseca, A.J.P., and Moura Costa Filho, L. 2013. Stiffness and strength governing the static liquefaction of tailings. *Journal of Geotechnical and Geoenvironmental Engineering*, ASCE.

Sotil, A., Soto, V., and Brouwer, K. 2020. Reducing long term risk at the Candelaria tailings storage facility. Proceedings of the 2020 Tailings and Mine Waste Conference. November 15-18, 2020.